

Assessing Contamination Sources by Using Sulfur and Oxygen Isotopes of Sulfate Ions in Xijiang River Basin, Southwest China

Guilin Han,* Yang Tang, Qixin Wu, Man Liu, and Zhengrong Wang

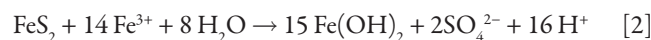
Abstract

The chemical and stable isotopic compositions ($\delta^{34}\text{S}_{\text{SO}_4}$ and $\delta^{18}\text{O}_{\text{SO}_4}$) of Xijiang River water in southwest China, were measured to determine the extent of rock weathering and associated CO_2 consumption rates, and to assess the contamination sources of river water. The SO_4^{2-} concentration in the river water was in the range of 0.05 to 0.96 mmol L^{-1} (mean value = 0.32 mmol L^{-1}) and was characterized by $\delta^{34}\text{S}_{\text{SO}_4}$ values ranging from -9.1 to 5.1‰ (mean value = -2.1‰) and $\delta^{18}\text{O}_{\text{SO}_4}$ values ranging from -0.4 to 10.8‰ (mean value = 5.0‰). The $\delta^{34}\text{S}_{\text{SO}_4}$ and $\delta^{18}\text{O}_{\text{SO}_4}$ values ranged from high to low from the upper reaches to the lower reaches in all the river water samples. The results indicate that the oxidation of sulfide and anthropogenic inputs are the dominant processes affecting SO_4^{2-} sources and S cycling of the Xijiang River during high-discharge conditions, which are controlled by regional hydrological processes that are affected by natural processes and anthropogenic inputs

Core Ideas

- The dual isotopes ($\delta^{34}\text{S}_{\text{SO}_4}$ and $\delta^{18}\text{O}_{\text{SO}_4}$) of sulfate indicated S sources.
- The weathering rates of carbonate and silicate were calculated.
- The relative contributions of various sources are identified.

RIVER SYSTEMS, an essential part of global biogeochemical cycle, carry vital fluxes from the continent to the ocean. Investigations of river water chemistry and isotopic composition allow us to understand chemical erosion processes and viable carbon dioxide (CO_2) consumption reservoirs, and to provide clues about the long-term climatic evolution (Negrel et al., 1993; Gaillardet et al., 1999; Millot et al., 2003; Xu and Liu, 2007; Han et al., 2010; Li and Ji, 2016). Previous studies suggested that silicate weathering regulates the greenhouse effect on a geological timescale (Walker et al., 1981; Gaillardet et al., 1999; Galy and France-Lanord, 1999; Han et al., 2016; Li and Ji, 2016). Moreover, the acidic solution produced during oxidation of sulfide to soluble sulfate (SO_4^{2-}) also plays an important role in weathering carbonate (Calmels et al., 2007; Li et al., 2008, 2013). Two main oxidation processes are involved in sulfide oxidation, including air oxygen (O_2) and iron (Fe^{3+}) (Li et al., 2014):



Both processes end up raising the alkalinity level of ocean, directly or indirectly affecting Earth's global carbon (C) cycle (Han and Liu, 2004; Spence and Telmer, 2005; Calmels et al., 2007; Li et al., 2011; Turchyn and DePaolo, 2011; Li et al., 2015; Li and Ji, 2016). Rapid urbanization and population growth in recent decades has increased the demand of metals. The excavation and extraction of metals from sulfide minerals have resulted in accelerated levels of water pollution and rock weathering rates, causing worldwide concern due to the potential impact on human societies (Shin et al., 2015). Thus, a quantitative understanding the riverine flux of sulfuric acid produced by oxidation of sulfide can offer additional constraints on carbonate and silicate weathering rates in terrestrial environments due to both natural and anthropogenic processes.

The dissolved SO_4^{2-} in river water could originate from several different sources, including precipitation, weathering of evaporite (e.g., gypsum and anhydrite), fertilizer, manure, sewage, or

© 2019 The Author(s). Re-use requires permission from the publisher.

J. Environ. Qual. 48:1507–1516 (2019)

doi:10.2134/jeq2019.03.0150

Supplemental material is available online for this article.

Received 31 Mar. 2019.

Accepted 25 June 2019.

*Corresponding author (hanguilin@cugb.edu.cn).

G. Han, M. Liu, and Z. Wang, Institute of Earth Sciences, China Univ. of Geosciences (Beijing), Beijing 10083, China; Y. Tang, The State Lab. of Environmental Geochemistry, Institute of Geochemistry, Chinese Academy of Sciences, Guiyang 550002, China; Q. Wu, Key Lab. of Karst Environment and Geohazard Prevention, Ministry of Education, Guizhou Univ., Guiyang 550003, China; Z. Wang, Dep. of Earth & Atmospheric Science, The City College of New York, CUNY, NY 10031, USA. Assigned to Associate Editor Samantha Ying.

Abbreviations: PC, principal component; PCA, principal component analysis.

soil organic matter. The chemical composition of surface water is insufficient to distinguish among these natural and anthropogenic sources, but isotopic compositions of sulfur (S) and oxygen (O) in SO_4^{2-} could potentially provide additional constraints to trace the sources and sinks of sulfate and reaction pathways (Calmels et al., 2007; Bottrell et al., 2008; Mayer et al., 2010; Yuan and Mayer, 2012; Li et al., 2013). For example, evaporite minerals such as gypsum and anhydrite are usually rich in heavy S and O isotopes ($\delta^{34}\text{S}_{\text{SO}_4}$ and $\delta^{18}\text{O}_{\text{SO}_4}$ ranging from ~ 10 to $\sim 30\text{‰}$; Claypool et al., 1980), whereas pyrite is more enriched in the light S isotope ($\delta^{34}\text{S}_{\text{SO}_4}$ ranging from 0 to -100‰ ; Heidel and Tichomirowa, 2011). Vitoria et al. (2004) and Szykiewicz et al. (2011) suggested that the $\delta^{34}\text{S}_{\text{SO}_4}$ of fertilizers ranges from -6.5 to $+11.7\text{‰}$ in the northern hemisphere.

Since the widespread combustion of coal in southwestern China, this study area is seriously impacted by sulfuric acid rain (Han and Liu, 2006; Han et al., 2011; Wu et al., 2012; Wu and Han, 2015). Previous studies have shown the influence of sulfuric acid on carbonate rock weathering in the upper reaches of the Xijiang River basin using $^{87}\text{Sr}/^{86}\text{Sr}$ and $\delta^{13}\text{C}_{\text{DIC}}$ (Xu and Liu, 2007; Li et al., 2008). Xu and Liu (2007) calculated the rock weathering rate by carbonic acid and by sulfuric acid, but they did not identify the sources of SO_4^{2-} of river water. Recent geochemical work indicated that sulfide-derived SO_4^{2-} fluxes were significantly underestimated in models of elemental cycles (Das et al., 2012). Here, we report new results for the composition of major elements and S and O isotope compositions of SO_4^{2-} in the Xijiang River. The main aims of the present study are to trace the sources of SO_4^{2-} and their apportionment in the Xijiang River basin, to understand the natural processes and anthropogenic inputs, and to estimate the chemical weathering rates and the related CO_2 consumption in the Xijiang River basin.

Materials and Methods

Study Area

The Pearl River (or Zhujiang River) basin is located in southwest China, between $21^\circ 31'$ and $26^\circ 49'$ N and $102^\circ 14'$ and $115^\circ 53'$ E. The water discharge of Pearl River is the second largest river system in China, second only to Changjiang River (PRWRC, 1991), and it is also the largest drainage system flowing into the South China Sea (Xu and Han, 2009). Moreover, the Pearl River delta is one of the most economically developed regions in China.

The Xijiang River is the main tributary of the Pearl River, which covers the Pearl River and provides $\sim 63.9\%$ of drainage and $\sim 77.8\%$ water discharge (Xu and Han, 2009). Xijiang River in Yunnan Province originates from Maxiong Mountain and flows through Guizhou, Guangxi, and Guangdong Provinces before entering the South China Sea (Fig. 1). Its basin is exposed to a subtropical monsoon climate, humid in summer.

Precambrian metamorphic rocks and Quaternary sediments are distributed in the Xijiang River basin (Fig. 1). Limestones, dolomites, and coal-bearing formations are exposed in the upper-middle reaches of the Xijiang River. Schists, gneiss, and granite are exposed in the middle-lower reaches of the Xijiang River. Shales and red sandstones are distributed in the source area and are fragmentarily intercalated in the middle basin area. Karst topography is well developed in the whole region.

Sampling and Analytical Procedures

A total of 81 river water samples were collected during the high flow discharge (15–31 July 2014) from the main channel and major tributaries of the Xijiang River. The sample numbers and sampling location are exhibited in Fig. 1.

River water samples were collected at water depths of about 0.5 to 1.0 m in the middle of the river on board a boat or on a bridge. The pH, water temperature, electric conductivity, and dissolved O_2 were immediately measured after sampling at each sampling site using a portable meter (WTW 3630). The bicarbonate (HCO_3^-) concentration was determined by titration with hydrochloric acid (HCl) in situ. All water samples were filtered through a $\sim 0.22\text{-}\mu\text{m}$ membrane after collection, and a portion of each sample was acidified with pure nitric acid (HNO_3) to $\text{pH} < 2$ after collection for measuring cations, whereas the other portion was stored for measuring anions.

The concentrations of major cations (sodium [Na^+], potassium [K^+], calcium [Ca^{2+}], and magnesium [Mg^{2+}]) and anions (chloride [Cl^-], nitrate [NO_3^-], and SO_4^{2-}) were measured by ion chromatography (Dionex, ICS 1100). The ammonium (NH_4^+) concentration was determined by spectrophotometry using the Nessler method (Krug et al., 1979), and silicon dioxide (SiO_2) concentration was determined by spectrophotometry. Reagent and procedural blanks were analyzed and treated by identical procedures as samples.

Analyses of S and O isotope compositions of the dissolved SO_4^{2-} ($\delta^{34}\text{S}_{\text{SO}_4}$ and $\delta^{18}\text{O}_{\text{SO}_4}$) were conducted on barium sulfate (BaSO_4) precipitated by mixing river water samples with 10% barium chloride (BaCl_2) solutions. After 48 h, the mixture was filtered through $\sim 0.22\text{-}\mu\text{m}$ membrane filters. The BaSO_4 sediment of filter will be carefully rinsed with Milli-Q water to remove Cl^- and then transferred to crucibles, under the temperature of 800°C in air combustion for 40 min (Han et al., 2016). The $\delta^{34}\text{S}_{\text{SO}_4}$ of BaSO_4 was determined on a Finnigan Delta-C isotope ratio mass spectrometer coupled with an elemental analyzer in a continuous-flow mode. Sulfur isotopic values were reported with respect to VCDT (Vienna-Canyon Diablo Troilite), and the $\delta^{34}\text{S}_{\text{SO}_4}$ value of the standard is $21.1 \pm 0.2\text{‰}$ ($n = 20$, 1σ) for NBS 127 (BaSO_4).

The $\delta^{18}\text{O}_{\text{SO}_4}$ value of BaSO_4 was measured in duplicates by online pyrolysis method using a ThermoQuest TC/EA unit coupled with a Finnigan Mat-Delta C mass spectrometer at the Institute of Geographic Sciences and Natural Resources Research, Chinese Academy of Sciences. The BaSO_4 was thermally decomposed in high reducing environment and the $\delta^{18}\text{O}$ value was analyzed on carbon monoxide (CO) gas carried by helium stream. The $\delta^{18}\text{O}_{\text{SO}_4}$ value of NBS 127 (BaSO_4) was measured to be $8.5 \pm 0.5\text{‰}$ ($n = 20$, 1σ).

Results

Water Chemistry

The field measurements, elemental analyses, and S and O isotope compositions of SO_4^{2-} , as well as statistical details of parameters, are summarized in Supplemental Table S1 and Table 1, the compositions of major ions are shown in Fig. 2, and their variations with distance from sources (Sampling Location 1 in Fig. 1) are depicted in Fig. 3.

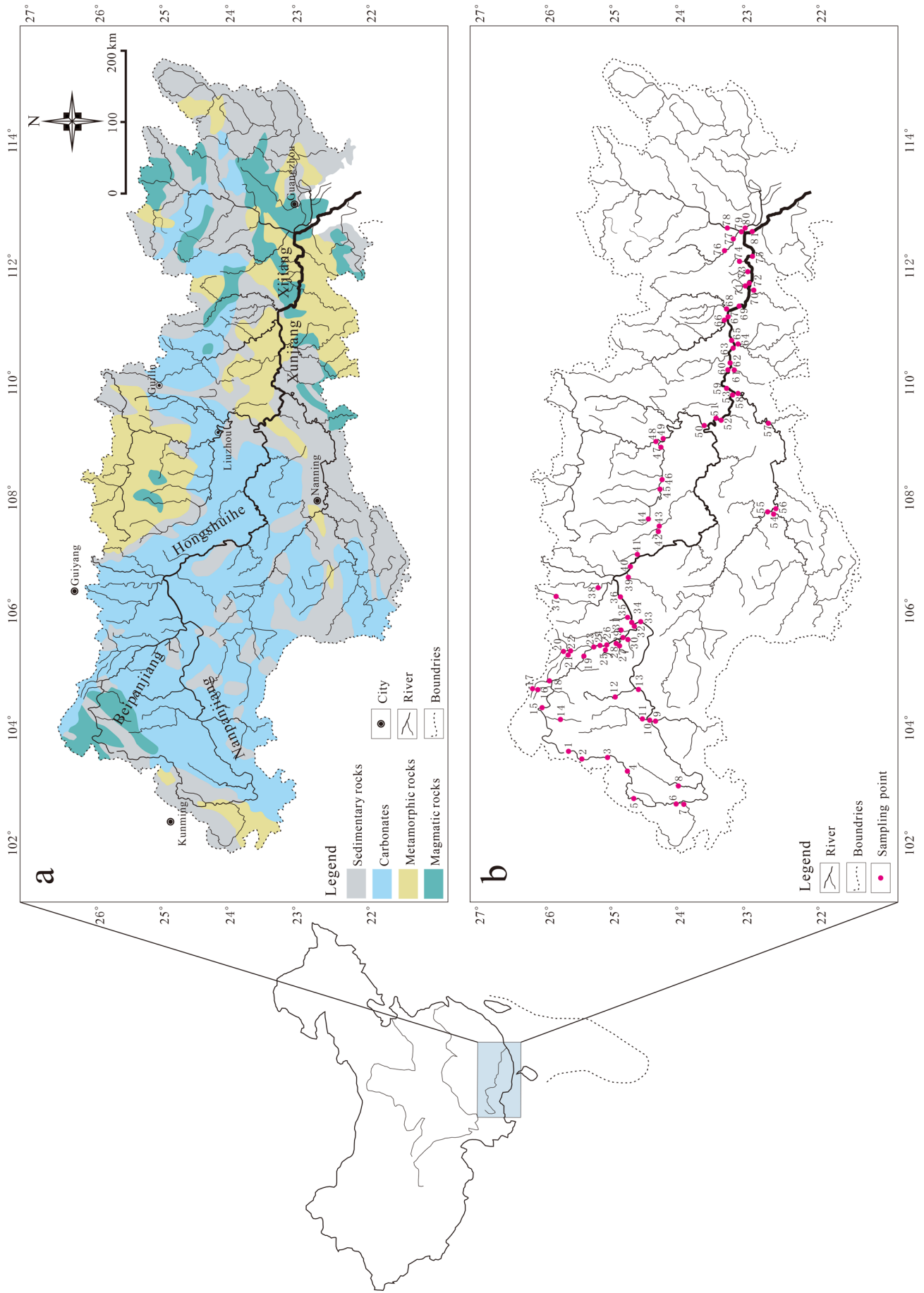


Fig. 1. (a) Sketch map showing the lithology of the Xijiang River. (b) Map showing sampling locations and sample numbers in the Xijiang River.

Table 1. Mean concentration (mmol/L) of major ionic compositions and pH (unit) along with statistical results in Xijiang River

Component	Mean	Median	SD	Min.	Max.
pH	7.7	7.7	0.4	6.4	8.4
Electrical conductivity ($\mu\text{S cm}^{-1}$)	153.8	159.5	57.1	45.0	266.5
Na^+ (mmol L ⁻¹)	0.17	0.14	0.11	0.02	0.56
K^+ (mmol L ⁻¹)	0.05	0.04	0.10	0.01	0.18
Mg^{2+} (mmol L ⁻¹)	0.30	0.27	0.18	0.07	0.07
Ca^{2+} (mmol L ⁻¹)	1.19	1.26	0.50	0.16	2.19
NH_4^+ (mmol L ⁻¹)	0.01	0.00	0.01	0.00	0.09
SiO_2 (mmol L ⁻¹)	0.15	0.11	0.22	0.00	1.69
HCO_3^- (mmol L ⁻¹)	2.09	1.18	0.83	0.28	3.65
Cl^- (mmol L ⁻¹)	0.13	0.10	0.10	0.03	0.56
NO_3^- (mmol L ⁻¹)	0.14	0.09	0.12	0.03	0.03
SO_4^{2-} (mmol L ⁻¹)	0.32	0.16	0.22	0.05	0.96
$\delta^{34}\text{S}$ (‰)	-2.05	-2.36	3.18	-9.06	5.06
$\delta^{18}\text{O}$ (‰)	4.95	5.13	3.10	-0.44	10.77

The pH value of river water samples varies from 6.4 to 8.4 (mean value = 7.7). The electrical conductivity varies from 45 to 267 $\mu\text{S cm}^{-1}$ (mean value = 155 $\mu\text{S cm}^{-1}$). Total dissolved salts (mg L⁻¹), expressed as the sum of the concentration of major inorganic ions ($\text{K}^+ + \text{Na}^+ + \text{Ca}^{2+} + \text{Mg}^{2+} + \text{NH}_4^+ + \text{SO}_4^{2-} + \text{Cl}^- + \text{NO}_3^- + \text{HCO}_3^-$), varies from 59 to 410 mg L⁻¹ (mean value = 235 mg L⁻¹). The normalized inorganic charge balance $[(\text{TZ}^+ - \text{TZ}^-)/\text{TZ}^-]$, where $\text{TZ}^- = 2\text{SO}_4^{2-} + \text{Cl}^- + \text{NO}_3^- + \text{HCO}_3^-$ is generally <10%, suggesting that the contribution of organic ligands to the charge balance is not significant (Gaillardet et al., 1997).

Variations of anion and cation concentrations in our water samples fall in a narrow band on ternary diagrams (Fig. 2). The cation content of our water samples is dominated by Ca^{2+} and Mg^{2+} (the Ca^{2+} concentration is typically higher than the Mg^{2+} concentration), which account for >80% of the total cation content (Fig. 2a). The dominant anion in our water samples is HCO_3^- (Fig. 2b), and the concentrations range from 0.28 to 3.70 mmol L⁻¹ (mean value = 2.11 mmol L⁻¹), followed by SO_4^{2-} , with a concentration ranging from 0.05 to 0.96 mmol L⁻¹ (mean value = 0.32 mmol L⁻¹). The HCO_3^- and SO_4^{2-} make up >90% of the total anion concentration in most samples.

Along the Xijiang River, Fig. 3a shows that the pH value of river water has significant oscillations in the upper and middle reaches (between 7.5 and 8.5), with sharp decreases at ~200

(Sample 5, pH = 7.6) and ~1000 km (Sample 40, pH = 7.7) from river source, but little change in the lower reaches (~7.5). The dissolved SO_4^{2-} concentration in the main channel is higher in the upstream area than that in the downstream area (Fig. 3b) and varies significantly in the upper and middle reaches between 0.2 and 0.6 mmol L⁻¹, but is relatively stable in the lower reaches (~0.12 mmol L⁻¹) except at ~1900 km (Sample 81, ~0.45 mmol L⁻¹).

$\delta^{34}\text{S}$ and $\delta^{18}\text{O}$ values of Sulfate in the River Water

The $\delta^{34}\text{S}_{\text{SO}_4}$ value of sulfate ranges from -3.2 to -4.6‰ in the main channel, and from -9.1 to -5.1‰ in the tributaries. The $\delta^{18}\text{O}_{\text{SO}_4}$ value of SO_4^{2-} ranges from 0.5 to 10.2‰ in the main channel, and from -0.4 to 10.8‰ in the tributaries. Along the Xijiang River, the $\delta^{34}\text{S}_{\text{SO}_4}$ value of sulfate decreases from ~4.5 to -4.0‰ in the first ~150 km, and then returned to ~5.1‰ between the upper and middle reaches. It gradually decreases to -4.1‰ at ~1000 km and slowly increases to lower reaches (Fig. 3c). The highest $\delta^{34}\text{S}_{\text{SO}_4}$ value of 5.1‰ is observed in the upper reaches, and then it decreases to -4.1‰. The $\delta^{18}\text{O}_{\text{SO}_4}$ value along the river also shows up 11‰ variation (Fig. 3d). It increases from 3.2 to 8.7‰ during the first 250 km of the river, decreases at the transition between the upper and middle reaches, gradually decreases from approximately 10.8 to -0.4‰ at ~800 to

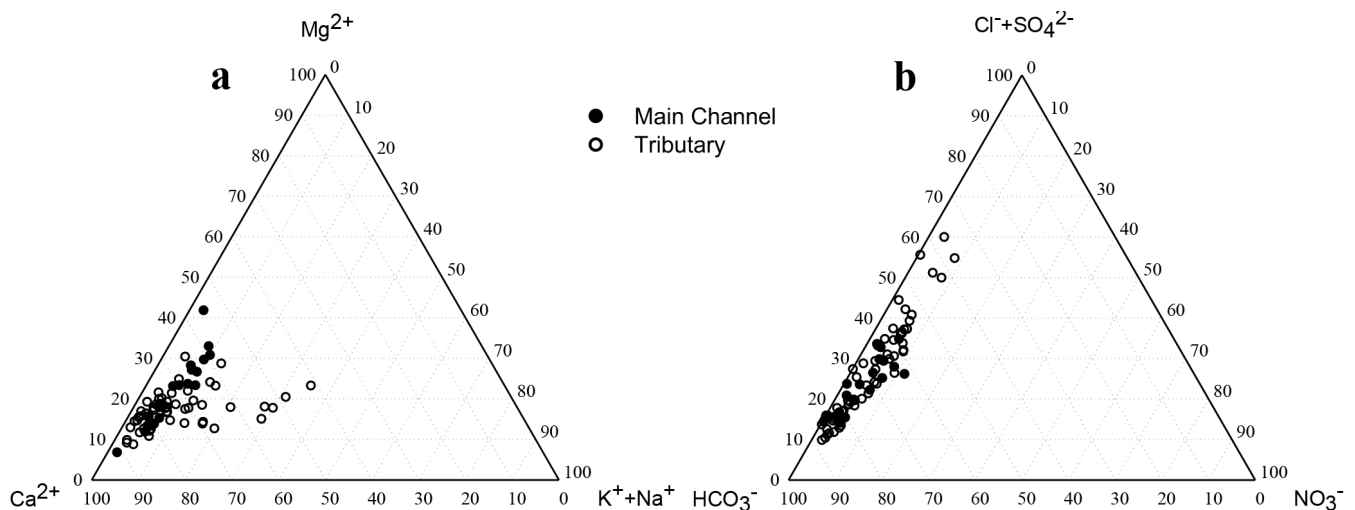


Fig. 2. Ternary diagram showing anion and cation compositions in the Xijiang River.

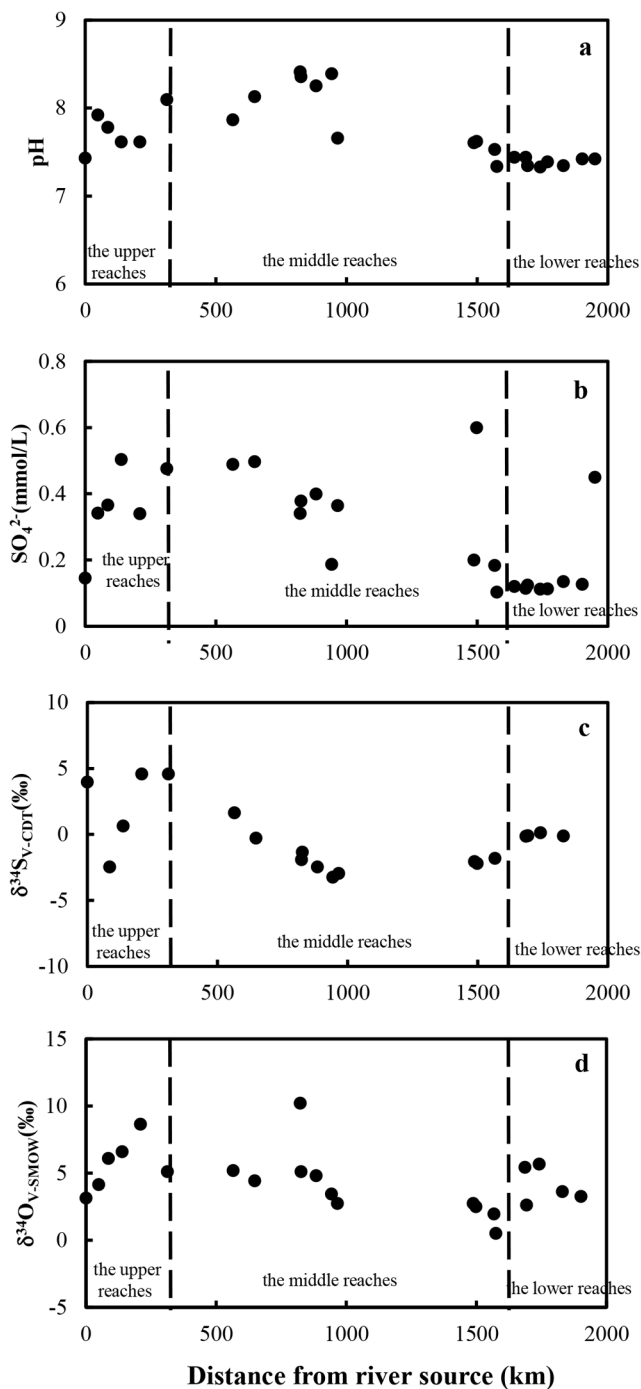


Fig. 3. The spatial variation of pH, SO_4^{2-} , $\delta^{34}\text{S}_{\text{V-CDT}}$, and $\delta^{18}\text{O}_{\text{V-SMOW}}$ in the river water of Xijiang River. V-CDT, Vienna Canyon Diablo Troilite; V-SMOW, Vienna Standard Mean Ocean Water.

~1600 km in the middle reaches, and then increases in the lower reaches. The $\delta^{18}\text{O}_{\text{SO}_4}$ value ranges from -0.4 to 10.8‰ (mean value = 5.0‰) in the whole catchment. These variations will be discussed in the section below.

Discussion

Potential Sources of Dissolved Sulfate

The principal component analysis (PCA) was conducted on our data to identify the origins of ions. The varimax-rotated PCA was performed by using SPSS 23.0 to reveal the relationships among all measured ions and isotopic compositions and

to help further determine the source allocation. Three principal components (PCs, eigenvalues >1) were extracted (Table 2), which account for a total $\sim 69.5\%$ and $\sim 76.5\%$ of the variance to the main channels and tributaries, respectively.

For the river water samples from the main channel, the first PC (PC1) explains $\sim 38.6\%$ of the total variance. The second PC (PC2) accounts for $\sim 18.4\%$ of the total variance and increases with increasing K^+ and Cl^- and decreasing Ca^{2+} , HCO_3^- , and pH values. When the charge of major ions is balanced, the pH values of the river water will be controlled by some minor components such as NO_3^- and Cl^- that are not balanced by other cations. The third PC (PC3) accounts for $\sim 12.4\%$ of the total variance and increased with increasing NH_4^+ , Na^+ , and SO_4^{2-} . This component could reflect the contribution of anthropogenic inputs.

For the tributaries, the PC1 explains $\sim 40.1\%$ of the total variance. The PC2 accounts for $\sim 19.3\%$ of the total variance and increases with increasing Cl^- and K^+ and decreasing Ca^{2+} , HCO_3^- , and pH values. The PC3 accounts for $\sim 9.8\%$ of the total variance and increased with increasing Na^+ and SO_4^{2-} . This component could reflect the contribution of anthropogenic inputs. The fourth PC (PC4) accounts for $\sim 7.2\%$ of the total variance and increased with increasing NH_4^+ . This component could reflect the contribution of another anthropogenic inputs. In summary, the PCs can be explained by the mixing of four major sources, including weathering of rock (carbonate and silicate), sulfide oxidation, and two kinds of human activities inputs.

Stoichiometry of River Waters

Figure 4 shows the covariation of $[\text{Ca}^{2+} + \text{Mg}^{2+}]/[\text{HCO}_3^-]$ versus $[\text{SO}_4^{2-}]/[\text{HCO}_3^-]$ (equivalent ratios), which show the likely chemical reactions for the chemical compositions of the river waters. All the river samples had equivalent ratios $[(\text{Ca}^{2+} + \text{Mg}^{2+})/\text{HCO}_3^-] > 1$, with a significant excess of Ca^{2+} and Mg^{2+} (Fig. 4). According to the stoichiometric relations of these chemical reactions, all samples have $[\text{Ca}^{2+} + \text{Mg}^{2+}]/[\text{HCO}_3^-] > 1$ and low $[\text{SO}_4^{2-}]/[\text{HCO}_3^-]$ ratios.

When carbonate minerals are dissolved and balanced by carbonic and sulfuric acids, $[\text{SO}_4^{2-}]/[\text{HCO}_3^-]$ equivalent ratio of water should be 0.5, and $[\text{Ca}^{2+} + \text{Mg}^{2+}]/[\text{HCO}_3^-]$ equivalent ratios of water should be 1.5. If the solute come from carbonate weathering by carbonic acid is mixed with gypsum dissolution, one of the two end-members should have a relative high $[\text{SO}_4^{2-}]/[\text{HCO}_3^-]$ equivalent ratio and $[\text{Ca}^{2+} + \text{Mg}^{2+}]/[\text{SO}_4^{2-}]$ equivalent ratio of 1, and the data points should fall near the gypsum dissolution line ($[(\text{Ca}^{2+} + \text{Mg}^{2+})/\text{SO}_4^{2-}] = 1$). The ratio of $[\text{Ca}^{2+} + \text{Mg}^{2+}]/[\text{HCO}_3^-]$ and $[\text{SO}_4^{2-}]/[\text{HCO}_3^-]$ equivalence of all samples was positively correlated, indicating that carbonate weathering solutes were mixed with carbonic acid and both carbonic and sulfuric acids. Most samples collected in the tributaries have higher $[\text{SO}_4^{2-}]/[\text{HCO}_3^-]$ ratios than those from main channel, indicating more involvement of sulfuric acid in the tributaries.

The SO_4^{2-} has been recognized as an important role in the ionic balance and rock weathering in Xijiang River (Xu and Liu, 2007; Li et al., 2008). According to Supplemental Table S1, from upper to lower reaches, the acidification of river water did not occur and the concentration of HCO_3^- decreased significantly in Xijiang River owing to the buffering effects of a large number of carbonate rocks in the whole catchment (Xu and Liu, 2007). One possible source of SO_4^{2-} may be the dissolution

Table 2. Fourteen physicochemical variables on three or four significant principle components (PCs) for river water samples.†

Variable	Main channel			Tributary			
	PC1	PC2	PC3	PC1	PC2	PC3	PC4
pH	0.77	-0.33	0.22	0.57	-0.50	0.29	0.13
Electrical conductivity	0.96	-0.03	-0.11	0.94	-0.18	-0.14	-0.01
Na ⁺	0.26	0.43	0.65	0.58	0.36	0.50	0.19
K ⁺	0.05	0.90	-0.11	0.51	0.79	-0.02	0.03
Mg ²⁺	0.87	0.28	-0.09	0.89	0.17	-0.01	0.04
Ca ²⁺	0.91	-0.14	-0.24	0.80	-0.37	-0.30	-0.05
NH ₄ ⁺	0.07	0.19	0.52	-0.17	0.08	0.04	0.90
SiO ₂	-0.56	0.38	0.10	-0.34	0.47	0.24	-0.30
HCO ₃ ⁻	0.78	-0.23	-0.47	0.74	-0.31	-0.51	-0.06
Cl ⁻	0.43	0.65	-0.38	0.70	0.57	-0.22	0.07
NO ₃ ⁻	0.73	0.36	0.11	0.83	0.15	0.12	-0.09
SO ₄ ²⁻	0.67	0.02	0.54	0.65	-0.31	0.50	-0.06
δ ³⁴ S	-0.39	0.45	-0.46	-0.08	0.74	-0.43	0.06
δ ¹⁸ O	0.03	0.63	0.07	0.28	0.43	0.36	-0.18
Variance (%)	38.65	18.43	12.41	40.14	19.34	9.78	7.23
Cumulative variance (%)	38.65	57.07	69.48	40.14	59.48	69.26	76.48

† Bold values indicate positive correlations.

of evaporite, but the source of SO₄²⁻ cannot be simply distinguished by stoichiometry.

According to the stoichiometry of river waters (Fig. 5), it is possible that a considerable amount of [Ca²⁺ + Mg²⁺] is balanced by SO₄²⁻. Assuming that SO₄²⁻ is only balanced by Ca²⁺ and Mg²⁺, the equilibrium [Ca²⁺ + Mg²⁺]* (where [Ca²⁺ + Mg²⁺]* = [Ca²⁺ + Mg²⁺] - [SO₄²⁻], equivalence) should be explained by the weathering of carbonate rocks and/or silicate rocks by carbonic acid. Similarly, assuming the balance of Na⁺ and K⁺, the equilibrium [Na⁺ + K⁺]* (where [Na⁺ + K⁺]* = [Na⁺ + K⁺] - [Cl⁻], equivalence) should be equalized amounts from carbonate and/or silicate weathering by carbonic acid. Figure 5 showed that most of the water sample points fell close to the intersection point near the two lines of [Mg²⁺ + Ca²⁺]*/[HCO₃⁻] = 1 and [Na⁺ + K⁺]*/[HCO₃⁻] = 0, respectively, indicating the dominance of carbonate weathering. Moreover, most water samples fall into the second quadrant, suggesting excess of both [Mg²⁺ + Ca²⁺]* and [Na⁺+K⁺]* over [HCO₃⁻], which indicates the existence of excessive cations in the river water. As a result, SO₄²⁻ in the river water is unlikely to come from evaporite dissolution, and we assume that it comes from atmospheric inputs, oxidation of sulfide minerals, and/or anthropogenic inputs.

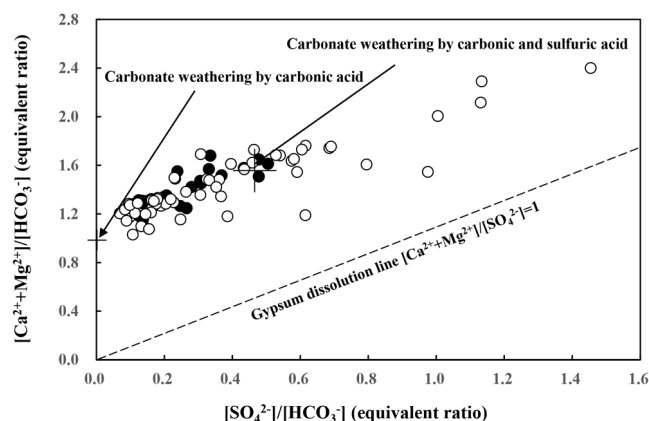


Fig. 4. Covariation of [Ca²⁺ + Mg²⁺]/[HCO₃⁻] vs. SO₄²⁻/HCO₃⁻ in the river water of Xijiang River. The symbols are the same as in Fig. 2.

Mixing Diagrams and Mixing Proportions

From our discussions above, because element cannot be distinguished among various components, isotopes thus can be used to identify the sources of river water. The isotopic compositions of δ³⁴S_{SO4} and δ¹⁸O_{SO4} have been used to identify different sources and trace the S cycle, including the inputs of human sulfate to river water (Spence and Telmer, 2005; Li et al., 2011). Evaporite mineral dissolution yields δ³⁴S_{SO4} values ranging between +8 and +35‰ and δ¹⁸O_{SO4} values ranging between +6 and +20‰, depending on the geological age (Li et al., 2013). We assess the potential contributions of different sources to the dissolved SO₄²⁻ in the sections below.

Atmospheric Inputs

The covariations of S and O isotopic ratios of SO₄²⁻ with 1/SO₄²⁻ are shown in Fig. 6. It can be observed that the δ³⁴S_{SO4} and δ¹⁸O_{SO4} values covered a wide range which was likely to be the result of the mixing of SO₄²⁻ contributions from natural and anthropogenic sources, rather than the variations of δ³⁴S_{SO4} from source rocks weathering within the basin. Krouse and Mayer (2000) suggested that δ³⁴S_{SO4} values of SO₄²⁻ from atmospheric

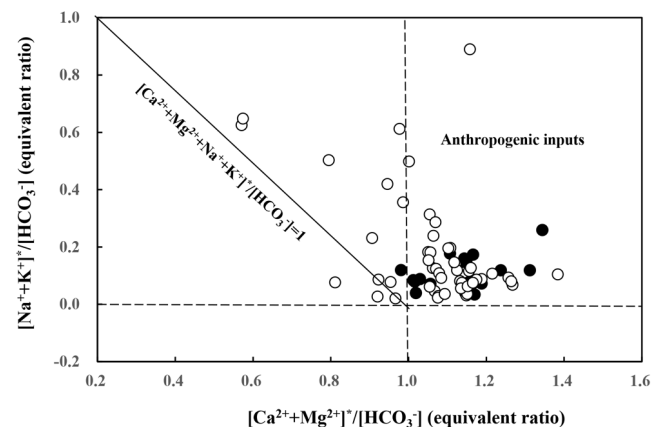


Fig. 5. Relative contributions from rock weathering by carbonic acid and anthropogenic inputs. For details, see the text. The symbols are the same as in Fig. 2.

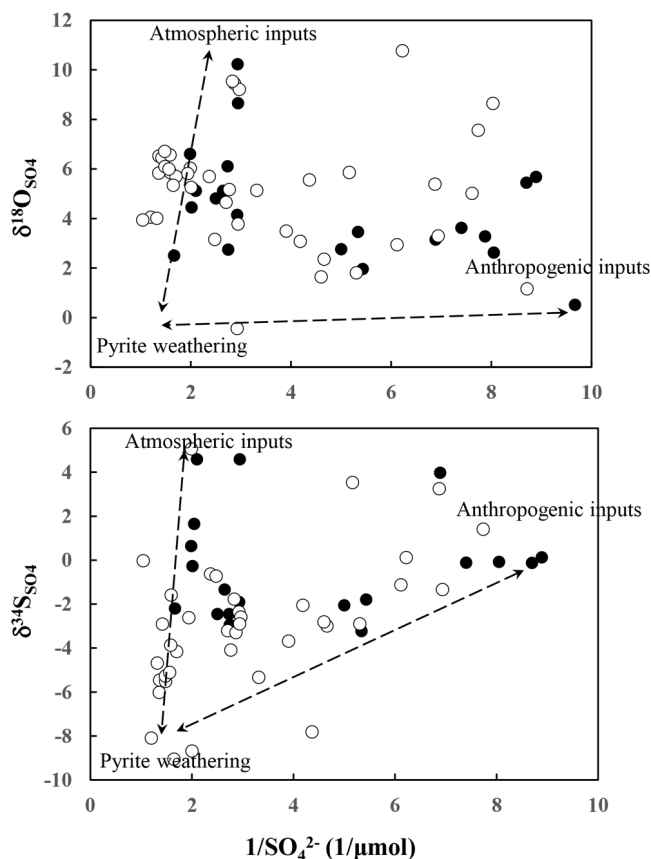


Fig. 6. Variation of $\delta^{34}\text{S}_{\text{SO}_4}$ and $\delta^{18}\text{O}_{\text{SO}_4}$ with $1/\text{SO}_4^{2-}$ molar ratios of the river waters.

deposition range from 0 to +6‰, and $\delta^{18}\text{O}_{\text{SO}_4}$ values of SO_4^{2-} range from +7 to +18‰, respectively. The $\delta^{34}\text{S}_{\text{SO}_4}$ values of rainwater in Guiyang City are reported to range from -12.0 to 9.4‰, with an average value of $-2.8 \pm 1.4\text{‰}$ (Xiao et al., 2011). To the best of our knowledge, no $\delta^{18}\text{O}_{\text{SO}_4}$ data for rainwater have been reported in southwestern China. According to our data, the highest $\delta^{34}\text{S}_{\text{SO}_4}$ value is 4.6‰ (Sample 37) and the highest $\delta^{18}\text{O}_{\text{SO}_4}$ value is 10.2‰ (Sample 33), and relatively high SO_4^{2-} may represent the atmospheric inputs in Xijiang River.

Oxidation of Sulfide

Evaporite dissolution yields of $\delta^{34}\text{S}_{\text{SO}_4}$ vary between +8 and +35‰, and yields of $\delta^{18}\text{O}_{\text{SO}_4}$ vary between +6 and +20‰, depending on the geological age (Claypool et al., 1980; Li et al., 2013). The variations in SO_4^{2-} plotted in the S and O isotope space are shown in Fig. 7. Most of the S and O isotope data in Xijiang River fall in the first quadrant, indicating that evaporite dissolution is not the main source. The oxidative weathering of pyrite, which provides dissolved SO_4^{2-} to river water, usually produces a negative $\delta^{34}\text{S}_{\text{SO}_4}$ values, which is consistent with the $\delta^{34}\text{S}_{\text{SO}_4}$ values we found in Xijiang River water samples.

In the Xijiang River basins, there is no geological evidence that evaporative strata exist, but there are extensive coal-containing strata exposed. Hong et al. (1993) reported that the S content of coal in Guizhou Province is high (average = 5.5%) and the value of $\delta^{34}\text{S}_{\text{SO}_4}$ is depleted (as low as -12.0 to -2.5‰, with a mean of -7.5‰), which considers that the SO_4^{2-} ions in river water do not mainly come from the gypsum dissolution. The typical $\delta^{18}\text{O}_{\text{SO}_4}$ values for the oxidation of reductive S range from

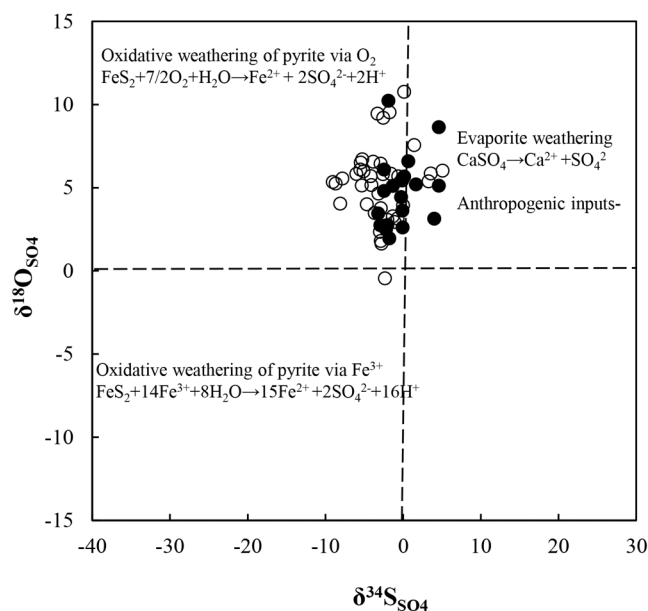


Fig. 7. A diagram of S-O isotope space showing that mineral weathering sources of riverine sulfate produce isotopically distinct sulfate.

-5.0 to 4.0‰ (Krouse and Mayer, 2000). According to our data (Fig. 6), the lowest $\delta^{34}\text{S}_{\text{SO}_4}$ value is -9.1‰ (Sample 12) and the lowest $\delta^{18}\text{O}_{\text{SO}_4}$ value is -0.5‰ (Sample 9), which may represent the oxidation of sulfide in Xijiang River. Therefore, the values of $\delta^{34}\text{S}_{\text{SO}_4}$ and $\delta^{18}\text{O}_{\text{SO}_4}$ of the oxidation of pyrite are considered to be -9.1 and -0.5‰ according to our data.

Anthropogenic Inputs

Previous studies have shown that SO_4^{2-} can originate from anthropogenic sources and the most likely candidates are agriculture and domestic and industrial wastes, which are known to supply SO_4^{2-} to river water (Vitoria et al., 2004; Li et al., 2011). The isotopic compositions of SO_4^{2-} of contamination sources for the river water collected in Xijiang River have not been measured, so the values from the literature can be used as references. The reported $\delta^{34}\text{S}_{\text{SO}_4}$ values from anthropogenic sources are as follows: (i) the $\delta^{34}\text{S}_{\text{SO}_4}$ of domestic wastes ranges from +8.5 to +13.6‰ (Vitoria et al., 2004); (ii) the $\delta^{34}\text{S}_{\text{SO}_4}$ of industrial wastewater ranges from +8.0 to +14.0‰ (Das et al., 2011); and (iii) the $\delta^{34}\text{S}_{\text{SO}_4}$ of fertilizers is around $4.0 \pm 4\text{‰}$ (Szykiewicz et al., 2011). Otero et al. (2007) suggested that the values of $\delta^{34}\text{S}_{\text{SO}_4}$ ranged from 0.0 to 5.0‰ and the $\delta^{18}\text{O}_{\text{SO}_4}$ values ranged between 3.8 and 6.0‰ in pig manure-contaminated groundwater. The $\delta^{34}\text{S}_{\text{SO}_4}$ value of sewage is reported to be about +9.6‰, whereas the $\delta^{18}\text{O}_{\text{SO}_4}$ value is about +10‰ (Otero et al., 2008). Because the $\delta^{34}\text{S}_{\text{SO}_4}$ and $\delta^{18}\text{O}_{\text{SO}_4}$ values of various contaminant sources in Xijiang River basin have not been characterized, it is difficult to identify the solutes for the anthropogenic input based on these references. It can be reasonably postulated that the anthropogenic end-member of Xijiang River according to our data (Fig. 6), Sample 9, has relatively low SO_4^{2-} ($0.11 \mu\text{mol L}^{-1}$) and the lowest $\delta^{18}\text{O}_{\text{SO}_4}$ value (-0.5‰) and should be the end-member of anthropogenic inputs; similarly, Sample 64 has a relatively low SO_4^{2-} value ($0.2 \mu\text{mol L}^{-1}$) and a relatively high $\delta^{34}\text{S}_{\text{SO}_4}$ value (0.1‰) and should be the end-member of anthropogenic inputs.

According to the discussion above regarding the sources of SO_4^{2-} in the Xijiang River, for the $\delta^{34}\text{S}_{\text{SO}_4}$ of the river water, a

balanced equation could be written based on the relative contributions of SO_4^{2-} from atmospheric inputs (F_{at}), the oxidation of sulfide minerals (F_{sulfide}), and anthropogenic inputs (F_{anthro}), and their $\delta^{34}\text{S}_{\text{SO}_4}$ and $\delta^{18}\text{O}_{\text{SO}_4}$ values can be expressed as follows, based on mass balance:

$$\delta^{34}\text{S}_{\text{SO}_4\text{riv}} = F_{\text{at}} \times \delta^{34}\text{S}_{\text{SO}_4\text{at}} + F_{\text{sulfide}} \times \delta^{34}\text{S}_{\text{SO}_4\text{sulfide}} + F_{\text{anthro}} \times \delta^{34}\text{S}_{\text{SO}_4\text{anthro}}$$

$$\delta^{18}\text{O}_{\text{SO}_4\text{riv}} = F_{\text{at}} \times \delta^{18}\text{O}_{\text{SO}_4\text{at}} + F_{\text{sulfide}} \times \delta^{18}\text{O}_{\text{SO}_4\text{sulfide}} + F_{\text{anthro}} \times \delta^{18}\text{O}_{\text{SO}_4\text{anthro}}$$

$$F_{\text{at}} + F_{\text{sulfide}} + F_{\text{anthro}} = 1$$

The end-members are as follows: $\delta^{34}\text{S}_{\text{SO}_4\text{at}} = 5.0\text{‰}$, $\delta^{18}\text{O}_{\text{SO}_4\text{at}} = 10.2\text{‰}$, $\delta^{34}\text{S}_{\text{SO}_4\text{sulfide}} = -9.1\text{‰}$, $\delta^{18}\text{O}_{\text{SO}_4\text{sulfide}} = -0.5\text{‰}$, $\delta^{34}\text{S}_{\text{SO}_4\text{anthro}} = 0.1\text{‰}$, $\delta^{18}\text{O}_{\text{SO}_4\text{anthro}} = -0.5\text{‰}$.

The fractions of SO_4^{2-} contributed by different sources (F_{at} , F_{sulfide} , and F_{anthro}) to the Xijiang River were estimated by using the various end-member values mentioned above (Fig. 8). From Fig. 8, it can be seen that the oxidation of sulfide ($\sim 45\%$) and atmospheric inputs ($\sim 32\%$) were the major sources of SO_4^{2-} in the tributaries of the Xijiang River. Anthropogenic inputs ($\sim 43\%$) and Oxidation of sulfide ($\sim 40\%$) were the major sources of SO_4^{2-} in the main channel of the Xijiang River. Using the upper and lower bounds of different SO_4^{2-} end-members in the mixed model, the absolute estimation error of the contributions of different sulfate sources is $\sim 40\%$.

Chemical Budget and Consequences for the Atmospheric Carbon Dioxide Budget

The S and O isotope compositions for sulfate ions from the Xijiang River were characterized by relatively low $\delta^{34}\text{S}_{\text{SO}_4}$ and $\delta^{18}\text{O}_{\text{SO}_4}$ values, indicating that SO_4^{2-} of river water is dominated by the oxidation of sulfide and anthropogenic inputs. As mentioned in the discussion above, the weathering of carbonates and silicates in the Xijiang River basin consumes sulfuric

acid produced by pyrite oxidation and sulfuric acid produced by human activities. Our calculations indicate that $\sim 43\%$ of the sulfuric acid involved in weathering reactions is from the oxidation of sulfide, whereas $\sim 31\%$ originates from the anthropogenic origin. This result implies that human activities can significantly accelerate rock weathering, especially in terrains where carbonate rocks are widely distributed. According to the classical viewpoint of the global C cycle (Berner and Kothavala, 2001), at steady state, the annual CO_2 consumption by the carbonate weathering process is compensated by the equivalent CO_2 emission from the ocean–atmosphere system during carbonate precipitation. However, previous studies (Berner et al., 1983; Calmels et al., 2007) noted that the cycle was not balanced when sulfuric acid is not considered in the weathering reactions. The weathering of carbonate by sulfuric acid can release CO_2 to the atmosphere, which is much more rapid than precipitation occurring in the ocean in the short term.

Previous studies have shown that sulfuric acid is very important to rock weathering (Galy and France-Lanord, 1999; Han and Liu, 2004; Spence and Telmer, 2005; Chetelat et al., 2008; Li et al., 2008; Han et al., 2010; Li and Ji, 2016). We estimated the chemical weathering rate of Xijiang (Supplemental Table S2; calculation are summarized in the supplemental material). According to China's 2014 river sediment bulletin (Ministry of Water Resources of the People's Republic of China, 2014), the discharge of Xijiang River is $227.2 \times 10^9 \text{ m}^3 \text{ yr}^{-1}$, and the silicate weathering rate was $9 \text{ t km}^{-2} \text{ yr}^{-1}$, which was higher than that of the Yangtze River basin (Chetelat et al., 2008). The mean weathering rate of carbonate by the combination of sulfuric and carbonic acid is $89 \text{ t km}^{-2} \text{ yr}^{-1}$, and the mean weathering rate of carbonate by carbonic acid is $68 \text{ t km}^{-2} \text{ yr}^{-1}$, which is higher than that of the world average weathering rate ($24 \text{ t km}^{-2} \text{ yr}^{-1}$; Gaillardet et al., 1999), Huanghe River ($26 \text{ t km}^{-2} \text{ yr}^{-1}$; Wu et al., 2008), and the Yangtze River ($65 \text{ t km}^{-2} \text{ yr}^{-1}$). Because the mean SO_4^{2-} concentration is $\sim 0.32 \text{ mmol L}^{-1}$, which is also the amount of CO_2 released into the atmosphere in an instant.

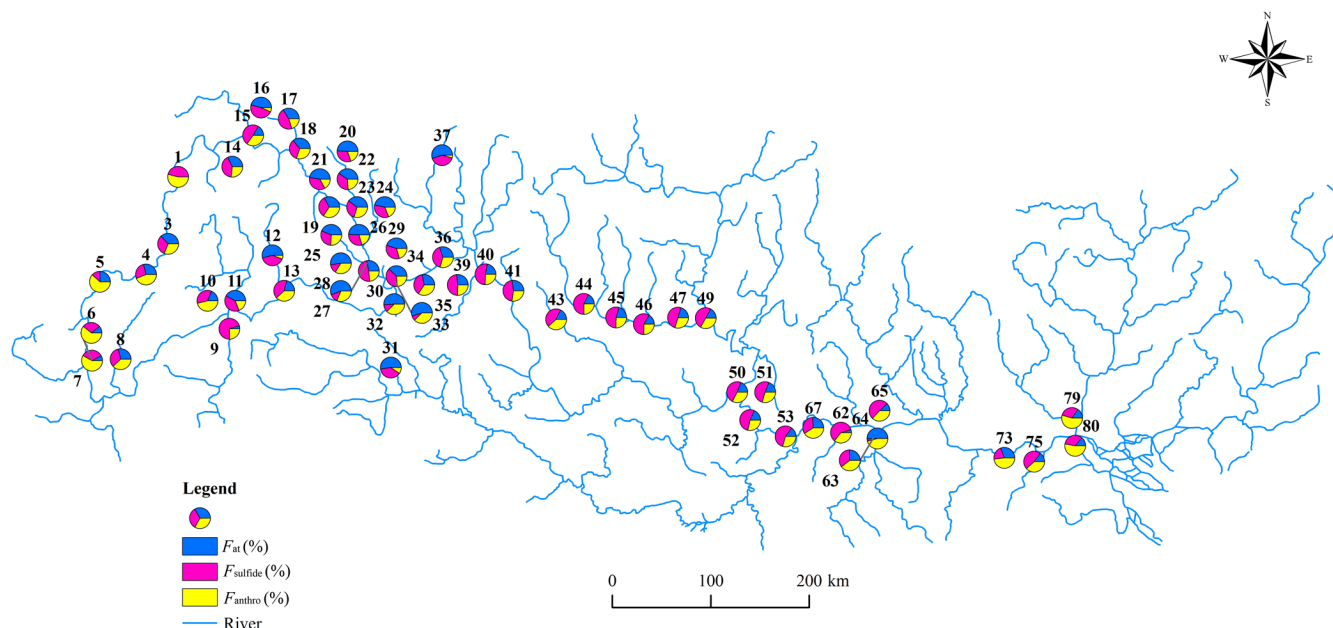


Fig. 8. The fractions of SO_4^{2-} contributed by different sources (F_{at} , F_{sulfide} , and F_{anthro}) to the Xijiang River, where F_{at} is atmospheric inputs, F_{sulfide} is the oxidation of sulfide minerals, and F_{anthro} is agricultural inputs.

According to the discharge of $227.2 \times 10^9 \text{ m}^3 \text{ yr}^{-1}$ for the Xijiang River basin, we calculated the consumption rate of CO_2 degassing of $426 \times 10^3 \text{ mol km}^{-2} \text{ yr}^{-1}$ by both sulfuric and carbonic acids, and $624 \times 10^3 \text{ mol km}^{-2} \text{ yr}^{-1}$ by carbonic acids. Compared with the weathering rate of carbonate under the action of carbonic acid alone, the higher weathering rate of carbonate by a combination of carbonic and sulfuric acid enhances weathering but decreases CO_2 consumption. Thus, the role of sulfuric acid in rock weathering should be taken into account in the local and even global C cycles.

Conclusions

In this study, the concentrations of the major ions, as well as S and O isotope data of sulfate were obtained riverine samples from the Xijiang River basin in southwest China. In most river samples, Ca^{2+} and Mg^{2+} accounted for >80% of the total cation concentration. Analyses of the stoichiometry of the river water indicate that $[\text{Ca}^{2+} + \text{Mg}^{2+}]$ is balanced by $[\text{SO}_4^{2-} + \text{HCO}_3^-]$, suggesting the importance of dissolving carbonate by a combination of sulfuric and carbonic acid.

The concentrations of SO_4^{2-} in the river water progressively decreased with the increase of flow distance, with the maximum concentration of 0.96 mmol L^{-1} in the upper reaches. The $\delta^{34}\text{S}_{\text{SO}_4}$ values in the river water ranged from -9.1 to 5.1‰ , with $\sim 90\%$ of the samples characterized by negative values. A gradual shift from higher to lower $\delta^{34}\text{S}_{\text{SO}_4}$ and $\delta^{18}\text{O}_{\text{SO}_4}$ values corresponded with the variation in SO_4^{2-} sources. The oxidation of sulfides, anthropogenic inputs, and atmospheric deposition were identified as major end-members and accounted for 45, 32, and 23% of the SO_4^{2-} in the tributaries, respectively. In the main channel, anthropogenic inputs oxidation of sulfide, and atmospheric inputs accounted for 43, 40, and 17% of the SO_4^{2-} , respectively. The results of this study show that sulfuric acid is an important factor in rock weathering reactions in Xijiang River. The oxidation of sulfide and anthropogenic inputs accounted for the enhanced weathering rates and exposed fresh mineral surfaces to chemically react with atmospheric O and water, consequently lowering CO_2 consumption. This suggests that the effect of sulfuric acid on rock weathering should be considered in the local, regional, and global C cycle.

Supplemental Material

This supporting information provides data as described in the manuscript. Supplemental Table S1 shows physicochemical and sulfate isotopic compositions in the river water of Xijiang during 2014. Supplemental Table S2 shows the calculation processes and results of chemical weathering and CO_2 consumption rate for the Xijiang River.

Conflict of Interest

The authors declare no conflict of interest.

Acknowledgments

This work was supported by the National Natural Science Foundation of China (Grant no. 41325010; 41661144029). The authors gratefully acknowledge Mr. Fushan Li and Yiliang Hou for field sampling.

References

Berner, R.A., A.C. Lasaga, and R.M. Garrels. 1983. The carbonate-silicate geochemical cycle and its effect on atmospheric carbon dioxide over the past 100 million years. *Am. J. Sci.* 283:641–683. doi:10.2475/ajs.283.7.641

- Berner, R.A., and Z. Kothavala. 2001. GEOCARB III: A revised model of atmospheric CO_2 over phanerozoic time. *Am. J. Sci.* 301:182–204. doi:10.2475/ajs.301.2.182
- Bottrell, S., J. Tellam, R. Bartlett, and A. Hughes. 2008. Isotopic composition of sulfate as a tracer of natural and anthropogenic influences on groundwater geochemistry in an urban sandstone aquifer, Birmingham, UK. *Appl. Geochem.* 23:2382–2394. doi:10.1016/j.apgeochem.2008.03.012
- Calmels, D., J. Gaillardet, A. Brenot, and C. France-Lanord. 2007. Sustained sulfide oxidation by physical erosion processes in the Mackenzie River basin: Climatic perspectives. *Geology* 35:1003–1006. doi:10.1130/G24132A.1
- Chetelat, B., C.Q. Liu, Z.Q. Zhao, Q.L. Wang, S.L. Li, J. Li, and B.L. Wang. 2008. Geochemistry of the dissolved load of the Changjiang basin rivers: Anthropogenic impacts and chemical weathering. *Geochim. Cosmochim. Acta* 72:4254–4277. doi:10.1016/j.gca.2008.06.013
- Claypool, G.E., W.T. Holser, I.R. Kaplan, H. Sakai, and I. Zak. 1980. The age curves of sulfur and oxygen isotopes in marine sulfate and their mutual interpretation. *Chem. Geol.* 28:641–683. doi:10.1016/0009-2541(80)90047-9
- Das, A., C.H. Chung, and C.F. You. 2012. Disproportionately high rates of sulfide oxidation from mountainous river basins of Taiwan orogeny: Sulfur isotope evidence. *Geophys. Res. Lett.* 39:L12404. doi:10.1029/2012GL051549
- Das, A., N.J. Pawar, and J. Veizer. 2011. Sources of sulfur in Deccan Trap rivers: A reconnaissance isotope study. *Appl. Geochem.* 26:301–307. doi:10.1016/j.apgeochem.2010.12.003
- Gaillardet, J., B. Dupre, C.J. Allegre, and P. Negrel. 1997. Chemical and physical denudation in the Amazon River basin. *Chem. Geol.* 142:141–173. doi:10.1016/S0009-2541(97)00074-0
- Gaillardet, J., B. Dupre, P. Louvat, and C.J. Allegre. 1999. Global silicate weathering and CO_2 consumption rates deduced from the chemistry of large rivers. *Chem. Geol.* 159:3–30. doi:10.1016/S0009-2541(99)00031-5
- Galy, A., and C. France-Lanord. 1999. Weathering processes in the Ganges-Brahmaputra basin and the riverine alkalinity budget. *Chem. Geol.* 159:31–60. doi:10.1016/S0009-2541(99)00033-9
- Han, G., and C. Liu. 2004. Water geochemistry controlled by carbonate dissolution: A study of the river waters draining karst-dominated terrain, Guizhou Province, China. *Chem. Geol.* 204:1–21. doi:10.1016/j.chemgeo.2003.09.009
- Han, G., and C. Liu. 2006. Strontium isotope and major ion chemistry of the rainwaters from Guiyang, Guizhou Province, China. *Sci. Total Environ.* 364:165–174. doi:10.1016/j.scitotenv.2005.06.025
- Han, G., Q. Wu, and Y. Tang. 2011. Acid rain and alkalization in southwestern China: Chemical and strontium isotope evidence in rainwater from Guiyang. *J. Atmos. Chem.* 68:139–155. doi:10.1007/s10874-012-9213-x
- Han, G., Y. Tang, and Z. Xu. 2010. Fluvial geochemistry of rivers draining karst terrain in Southwest China. *J. Asian Earth Sci.* 38:65–75. doi:10.1016/j.jseas.2009.12.016
- Han, X., Q. Guo, C. Liu, P. Fu, H. Strauss, J. Yang, et al. 2016. Using stable isotopes to trace sources and formation processes of sulfate aerosols from Beijing, China. *Sci. Rep.* 6:29958. doi:10.1038/srep29958
- Heidel, C., and M. Tichomirowa. 2011. The isotopic composition of sulfate from anaerobic and low oxygen pyrite oxidation experiments with ferric iron: New insights into oxidation mechanisms. *Chem. Geol.* 281:305–316. doi:10.1016/j.chemgeo.2010.12.017
- Hong, Y., H. Zhang, and Y. Zhu. 1993. Sulfur isotopic characteristics of coal in China and sulfur isotopic fractionation during coal-burning process. *Chin. J. Geochem.* 12:51–59. doi:10.1007/BF02869045
- Krouse, H.R., and B. Mayer. 2000. Sulphur and oxygen isotopes in sulphate. In: P.G. Cook and A.L. Herczeg, editors, *Environmental tracers in subsurface hydrology*. Kluwer Acad., Boston, MA. doi:10.1007/978-1-4615-4557-6_7
- Krug, F.J., J. Ruzicka, and E.H. Hansen. 1979. Determination of ammonia in low concentrations with Essler's reagent by flow injection analysis. *Analyst* 104:47–54. doi:10.1039/an9790400047
- Li, C., and H. Ji. 2016. Chemical weathering and the role of sulfuric and nitric acids in carbonate weathering: Isotopes ($\delta^{13}\text{C}$, $\delta^{15}\text{N}$, $\delta^{34}\text{S}$, and $\delta^{18}\text{O}$) and chemical constraints. *J. Geophys. Res.: Biogeosci.* 121:1288–1305. doi:10.1002/2015JG003121
- Li, S.-L., D. Calmels, G. Han, J. Gaillardet, and C.-Q. Liu. 2008. Sulfuric acid as an agent of carbonate weathering constrained by $\delta^{13}\text{C}_{\text{DIC}}$: Examples from Southwest China. *Earth Planet. Sci. Lett.* 270:189–199. doi:10.1016/j.epsl.2008.02.039
- Li, S.-L., B. Chetelat, F. Yue, Z. Zhao, and C.-Q. Liu. 2014. Chemical weathering processes in the Yalong River draining the eastern Tibetan Plateau, China. *J. Asian Earth Sci.* 88:74–84. doi:10.1016/j.jseas.2014.03.011
- Li, X., Y. Gan, A. Zhou, and Y. Liu. 2015. Relationship between water discharge and sulfate sources of the Yangtze River inferred from seasonal variations of sulfur and oxygen isotopic compositions. *J. Geochem. Explor.* 153:30–39. doi:10.1016/j.gexplo.2015.02.009

- Li, X., Y. Gan, A. Zhou, Y. Liu, and S. Wang. 2013. Hydrological controls on the sources of dissolved sulfate in the Heihe River, a large inland river in the arid northwestern China, inferred from S and O isotopes. *Appl. Geochem.* 35:99–109. doi:10.1016/j.apgeochem.2013.04.001
- Li, X.-D., C.-Q. Liu, X.-L. Liu, and L.-R. Bao. 2011. Identification of dissolved sulfate sources and the role of sulfuric acid in carbonate weathering using dual-isotopic data from the Jialing River, Southwest China. *J. Asian Earth Sci.* 42:370–380. doi:10.1016/j.jseas.2011.06.002
- Mayer, B., J.B. Shanley, S.W. Bailey, and M.J. Mitchell. 2010. Identifying sources of stream water sulfate after a summer drought in the Sleepers River watershed (Vermont, USA) using hydrological, chemical and isotopic techniques. *Appl. Geochem.* 25:747–754. doi:10.1016/j.apgeochem.2010.02.007
- Millot, R., J. Gaillardet, and C.J. Allegre. 2003. Northern latitude chemical weathering rates: Clues from the Mackenzie River basin, Canada. *Geochim. Cosmochim. Acta* 67:1305–1329. doi:10.1016/S0016-7037(02)01207-3
- Ministry of Water Resources of the People's Republic of China. 2014. China's 2014 river sediment bulletin 2014. Minist. Water Resour. People Repub. China, Beijing.
- Negrel, P., C.J. Allegre, B. Dupre, and E. Lewin. 1993. Erosion sources determined by inversion of major and trace element ratios and strontium isotopic ratios in river water: The Congo basin case. *Earth Planet. Sci. Lett.* 120:59–76. doi:10.1016/0012-821X(93)90023-3
- Otero, N., A. Canals, and A. Soler. 2007. Using dual-isotope data to trace the origin and processes of dissolved sulphate: A case study in Calders stream (Llobregat basin, Spain). *Aquat. Geochem.* 13:109–126. doi:10.1007/s10498-007-9010-3
- Otero, N., A. Soler, and A. Canals. 2008. Controls of $\delta^{34}\text{S}$ and $\delta^{18}\text{O}$ in dissolved sulphate: Learning from a detailed survey in the Llobregat River (Spain). *Appl. Geochem.* 23:1166–1185. doi:10.1016/j.apgeochem.2007.11.009
- Pearl River Water Resources Committee (PRWRC). 1991. The Zhujiang archive. Vol. 1. (In Chinese.) Guangdong Sci. Technol. Press, Guangzhou, China.
- Shin, W.J., J.S. Ryu, K.S. Lee, and Y. Park. 2015. Identification of anthropogenic contaminant sources in urbanized streams using multiple isotopes. *Environ. Earth Sci.* 73:8311–8324. doi:10.1007/s12665-014-3992-0
- Spence, J., and K. Telmer. 2005. The role of sulfur in chemical weathering and atmospheric CO_2 fluxes: Evidence from major ions, $\delta^{13}\text{C}_{\text{DIC}}$, and $\delta^{34}\text{S}_{\text{SO}_4}$ in rivers of the Canadian Cordillera. *Geochim. Cosmochim. Acta* 69:5441–5458. doi:10.1016/j.gca.2005.07.011
- Szynkiewicz, A., J.C. Witcher, M. Modelska, D.M. Borrok, and L.M. Pratt. 2011. Anthropogenic sulfate loads in the Rio Grande, New Mexico (USA). *Chem. Geol.* 283:194–209. doi:10.1016/j.chemgeo.2011.01.017
- Turchyn, A.V., and D.J. DePaolo. 2011. Calcium isotope evidence for suppression of carbonate dissolution in carbonate-bearing organic-rich sediments. *Geochim. Cosmochim. Acta* 75:7081–7098. doi:10.1016/j.gca.2011.09.014
- Vitoria, L., N. Otero, A. Soler, and A. Canals. 2004. Fertilizer characterization: Isotopic data (N, S, O, C and Sr). *Environ. Sci. Technol.* 38:3254–3262. doi:10.1021/es0348187
- Walker, J.C.G., P.B. Hays, and J.F. Kasting. 1981. A negative feedback mechanism for the long-term stabilization of Earth's surface temperature. *J. Geophys. Res. Oceans* 86:9776–9782. doi:10.1029/JC086iC10p09776
- Wu, Q., and G. Han. 2015. Sulfur isotope and chemical composition of the rainwater at the Three Gorges Reservoir. *Atmos. Res.* 115:130–140. doi:10.1016/j.atmosres.2014.11.020
- Wu, Q., G. Han, F. Tao, and Y. Tang. 2012. Chemical composition of rainwater in a karstic agricultural area, Southwest China: The impact of urbanization. *Atmos. Res.* 111:71–78. doi:10.1016/j.atmosres.2012.03.002
- Wu, W., S. Xu, J. Yang, and H. Yin. 2008. Silicate weathering and CO_2 consumption deduced from the seven Chinese rivers originating in the Qinghai-Tibet Plateau. *Chem. Geol.* 249:307–320. doi:10.1016/j.chemgeo.2008.01.025
- Xiao, H.W., H.Y. Xiao, and A.M. Long. 2011. Sulfur isotopic geochemical characteristics in precipitation at Guiyang. (In Chinese.) *Geochimica* 40:559–565. doi:10.19700/j.0379-1726.2011.06.007
- Xu, Z., and C. Liu. 2007. Chemical weathering in the upper reaches of Xijiang River draining the Yunnan-Guizhou Plateau, Southwest China. *Chem. Geol.* 239:83–95. doi:10.1016/j.chemgeo.2006.12.008
- Xu, Z., and G. Han. 2009. Rare earth elements (REE) of dissolved and suspended loads in the Xijiang River, South China. *Appl. Geochem.* 24:1803–1816. doi:10.1016/j.apgeochem.2009.06.001
- Yuan, F., and B. Mayer. 2012. Chemical and isotopic evaluation of sulfur sources and cycling in the Pecos River, New Mexico, USA. *Chem. Geol.* 291:13–22. doi:10.1016/j.chemgeo.2011.11.014